

Project no.:

608608

Project acronym:

MiReCOL

Project title:

Mitigation and remediation of leakage from geological storage

Collaborative Project

Start date of project: 2014-03-01

Duration: 3 years

D4.4

Brine/water withdrawal as pressure management and flow diversion option for a CO₂ storage operation

Status: definitive

Organisation name of lead contractor for this deliverable:

IMPERIAL

Project co-funded by the European Commission within the Seventh Framework Programme		
Dissemination Level		
PU	Public	X
PP	Restricted to other programme participants (including the Commission Services)	
RE	Restricted to a group specified by the consortium (including the Commission Services)	
CO	Confidential , only for members of the consortium (including the Commission Services)	

Deliverable number:	D4.4
Deliverable name:	Brine/water withdrawal as pressure management and flow diversion option for a CO ₂ storage operation
Work package:	WP4: Reservoir pressure management as CO ₂ migration and remediation measure
Lead contractor:	GFZ

Status of deliverable		
Action	By	Date
Submitted (Author(s))	Rajesh Govindan	October 2016
	Zhenggang Nie	October 2016
	Sevket Durucan	November 2016
	Anna Korre	October 2016
Approved by project leader	Holger Cremer	16 Jan. 2017

Author(s)		
Name	Organisation	E-mail
Rajesh Govindan	Imperial College	r.govindan07@imperial.ac.uk
Zhenggang Nie	Imperial College	zhenggang.nie04@imperial.ac.uk
Sevket Durucan	Imperial College	s.durucan@imperial.ac.uk
Anna Korre	Imperial College	a.korre@imperial.ac.uk

Abstract
<p>This report is part of the research project MiReCOL (Mitigation and Remediation of CO₂ leakage) funded by the EU FP7 programme. Research activities aim at developing a handbook of corrective measures that can be considered in the event of undesired migration of CO₂ in the deep subsurface reservoirs. MiReCOL results support CO₂ storage project operators in assessing the value of specific corrective measures if the CO₂ in the storage reservoir does not behave as expected. MiReCOL focuses on corrective measures that can be taken while the CO₂ is in the deep subsurface. The general scenarios considered in MiReCOL are 1) loss of conformance in the reservoir (undesired migration of CO₂ within the reservoir), 2) natural barrier breach (CO₂ migration through faults or fractures), and 3) well barrier breach (CO₂ migration along the well bore).</p> <p>This element of the MiReCOL project aims to investigate the feasibility of brine withdrawal technique and test its effectiveness for pressure management and CO₂ flow diversion in a storage reservoir. The study uses a field-scale reservoir model of the P18-A block, which represents a group of three depleted gas fields, namely the P18-2, P18-4 and P18-6 fields, located in the Dutch offshore region, 20 km north-west of Rotterdam, at an average depth of 3,500m below sea level. The model was made available by TNO in the MiReCOL project model database. Three scenarios were investigated by selecting the largest field in the block, namely the P18-2 field, which is broadly divided into three compartments. The results obtained using the CO₂ injection and brine production simulations were individually analysed and the key performance indicators (KPIs) for each scenario, namely: (a) well layouts for remediation; (b) volume of extracted brine; (c) longevity of remediation; (d) response time of remediation; (e) spatial extension of remediation; and (f) the estimated costs of remediation, are summarised in this report.</p>

TABLE OF CONTENTS

		Page
1	INTRODUCTION.....	2
1.1	Review of the application of reservoir brine production in CO ₂ storage	2
1.2	Objectives of the study	3
2	DESCRIPTION OF THE STUDY AREA.....	4
2.1	P18-A block.....	4
2.1.1	<i>Structural history</i>	5
2.1.2	<i>Reservoir geology</i>	5
2.2	P18-A reservoir model	6
2.2.1	<i>Structural and geological model</i>	6
2.2.2	<i>Dynamic properties of the reservoir model</i>	7
3	CO ₂ FLOW DIVERSION AND PRESSURE MANAGEMENT IN THE RESERVOIR WITH BRINE WITHDRAWAL	8
3.1	CO ₂ injection: plume migration and pressure analyses	8
3.1.1	<i>Compartment P18-2 (1)</i>	9
3.1.2	<i>Compartment P18-2 (2)</i>	12
3.1.3	<i>Compartment P18-2 (3)</i>	14
3.2	Relaxation of the reservoir	17
3.2.1	<i>Compartment P18-2 (1)</i>	18
3.2.2	<i>Compartment P18-2 (2)</i>	19
3.2.3	<i>Compartment P18-2 (3)</i>	20
3.3	Brine withdrawal	21
3.3.1	<i>Compartment P18-2 (1)</i>	21
3.3.2	<i>Compartment P18-2 (2)</i>	22
3.3.3	<i>Compartment P18-2 (3)</i>	23
3.3.4	<i>Summary of the key performance indicators</i>	24
4	CONCLUSIONS	26
5	REFERENCES	27

1 INTRODUCTION

A number of risks are associated with the underground storage of CO₂. The risks are mechanisms that could lead to the migration of CO₂ outside the storage complex, into the shallower formations, and ultimately resulting in surface emissions to the atmosphere. These include CO₂ leakage through: (a) sub-seismic faults that were undetected during the site characterisation phase prior to injection; (b) geomechanical effects, such as the reactivation of faults and the creation of new fractures in the caprock due to reservoir over-pressure created during injection (Rutqvist *et al.*, 2007, 2008); (c) presence of improperly plugged abandoned wells in the field (Carroll *et al.*, 2009; Zheng *et al.*, 2009; Apps *et al.*, 2010); and (d) geochemical reactions between CO₂ and the caprock (IEAGHG Report, 2007). In particular, over-pressurisation of the reservoir is of concern because it could have a large-scale impact, namely interference with the operations in neighbouring oil and gas fields, or CO₂ storage sites that could co-exist in the same formation. Such interference also has regulatory implications since issuing permits to operators would then be based on the outcome of a multi-site process evaluation, which can be quite involved, and rather unnecessary (Birkholzer and Zhou, 2009).

In view of the potential risks, contingency planning and analysis of leakage remediation is thus a requirement in order for the operator to obtain a permit for CO₂ storage. Some of the remediation options that were investigated in the current MiReCOL project include: (a) injection of sealant materials, such as polymer-gel solutions to create a localised reduction in permeability, either inside the reservoir or above the caprock, in order to divert the migration of the plume; (b) injection of brine in the reservoir to create a competitive fluid movement or enhance CO₂ dissolution; (c) injection of brine in a high permeability formation above the caprock in order to create a pressure (hydraulic) barrier; and (d) production of brine from the reservoir in order to regulate its pressure during injection, enhance the efficiency of CO₂ storage (or capacity utilisation), and possibly induce plume steering.

1.1 Review of the application of reservoir brine production in CO₂ storage

Benson and Hepple (2005) investigated scenarios wherein the leakage of CO₂ through various pathways, such as faults and fractures, were modelled. It was demonstrated that by producing brine from the reservoir, the pressure-driven leakage was minimised and consequently the net of amount of leakage is largely buoyancy-driven, thus reducing the rate of leakage. While pressure management via brine extraction is not be considered a mandatory component for large-scale CO₂ storage projects, it could also potentially provide many other benefits, such as increased storage capacity utilisation, simplified permitting, smaller area of review for site monitoring, and the manipulation of CO₂ plume in order to increase its sweep efficiency (Birkholzer *et al.*, 2012).

Buscheck *et al.* (2011) coined the acronym 'ACRM', which stands for active CO₂ reservoir management, wherein CO₂ injection is combined with simultaneous brine production for the storage in saline formations. The specific reservoir performance objectives of ACRM are to relieve pressure build-up, increase CO₂ injectivity, increase available pore space and storage capacity, manipulate CO₂ migration, and constrain brine migration. In summary, ACRM enables greater control of subsurface fluid migration and pressure perturbations. Additionally, Buscheck *et al.* (2012) provide a qualitative overview of the subsequent options to handle the produced brine, including desalination, saline water for cooling the towers at the CO₂ capture facility, source of makeup water for enhanced oil recovery (EOR) systems, and geothermal energy production. Various industries provide evidence that brine-sourced heat, minerals, and water are

marketable products that present an opportunity for considering the brine as a resource (Breunig *et al.*, 2013).

In terms of plume steering, the use of brine production has been analysed for CO₂ injection from a single vertical well surrounded by a ring of vertical brine production wells (Buscheck *et al.*, 2011; Court *et al.*, 2011). Court *et al.* (2011) found a single ring of four vertical production wells, has a negligible steering potential on the CO₂ plume and concluded that complex well placement strategies would need to be devised. On the other hand, Buscheck *et al.* (2011) showed significant steering potential with the availability of many more brine producing wells in the neighbourhood. However, this option is economically viable for depleted oil and gas reservoirs that could have a myriad of exploration and hydrocarbon production wells.

Buscheck *et al.* (2011) also showed that by extracting brine from the lower portion of the storage formation, much of the buoyancy force that tends to drive CO₂ to the top of the storage formation is counteracted, thereby higher storage efficiency is obtained, and injectivity is improved. However, Bergmo *et al.* (2011) concluded that in order to utilise an additional fraction of 1-2% of the pore volume for CO₂ storage, it is necessary to produce significant amounts of brine from the reservoir.

Another important aspect in brine production is considering the possibility of eventual CO₂ breakthrough at brine production wells (Buscheck *et al.*, 2012). Therefore, the general challenge for brine production is to determine the operational parameters, such as the number, location and type (vertical or horizontal) of wells, spacing between the wells, and the corresponding rates of brine production so that while the targeted pressure relief is achieved, CO₂ breakthrough time is also delayed. Solving this trade-off requires separate process-optimisation studies in order to determine the best CO₂ injection-brine production strategy, including cost optimisation, for each storage site that is selected.

1.2 Objectives of the study

The objectives of the study described in this report is to perform numerical modelling of brine withdrawal technique and test its effectiveness for pressure management and CO₂ flow diversion in a storage reservoir. Different scenarios were considered to determine the key performance indicators (KPIs) of the technique under the scope of the MiReCOL project, namely: (a) well layouts for remediation; (b) volume of extracted brine; (c) longevity of remediation; (d) response time of remediation; (e) spatial extension of remediation; and (f) the estimated costs of remediation.

In particular, the study area and the reservoir model characteristics are described in section 0. It is one of many models in the MiReCOL project model database, and represents an offshore and compartmentalised depleted gas reservoir. In section 0, the scenarios considered are described and the results and their KPI analyses are presented. The conclusions from this study and some recommendation for future work are made in section 0.

2 DESCRIPTION OF THE STUDY AREA

2.1 P18-A block

The P-18A block represents a group of three depleted gas fields, namely the P18-2, P18-4 and P18-6 fields, located in the Dutch offshore region, 20 km north-west of Rotterdam, at an average depth of 3,500m below sea level. The clastic reservoir rocks in these fields form a part of the Triassic Main Buntsandstein Subgroup with a disconformably overlying primary seal comprising of siltstones, clay stones, evaporates and dolostones. The gas fields are heavily faulted, hence forming hydraulically isolated compartments that are either fully or partially closed to their surroundings, as illustrated in Figure 1.

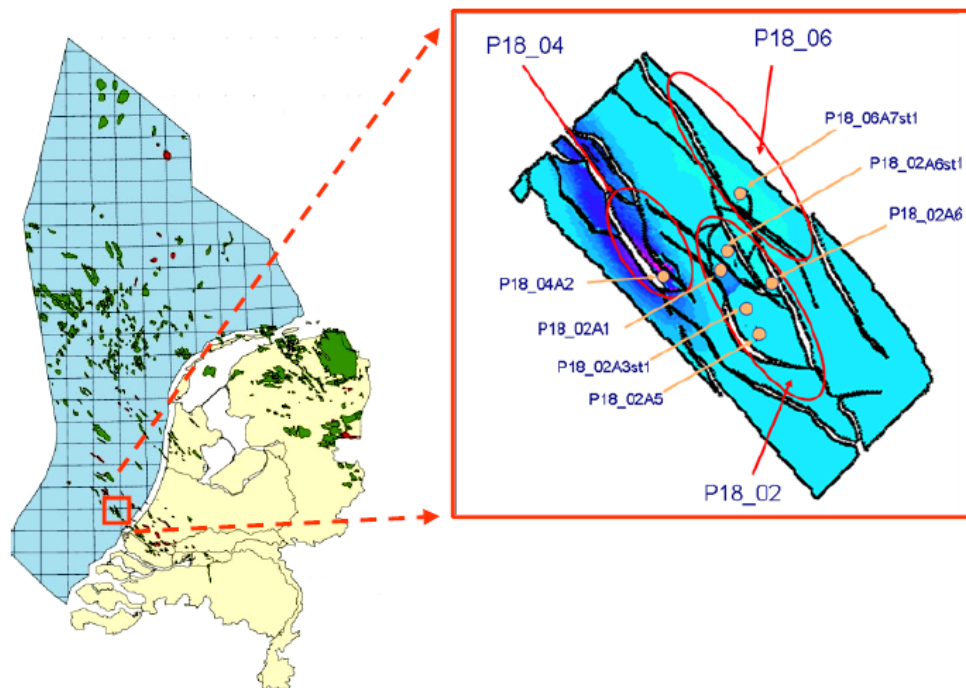


Figure 1 The offshore location of the P18-A block, comprising of the depleted gas fields P18-2, P18-4 and P18-6 (after Gutierrez-Neri *et al.* (2012), the CATO-2 project).

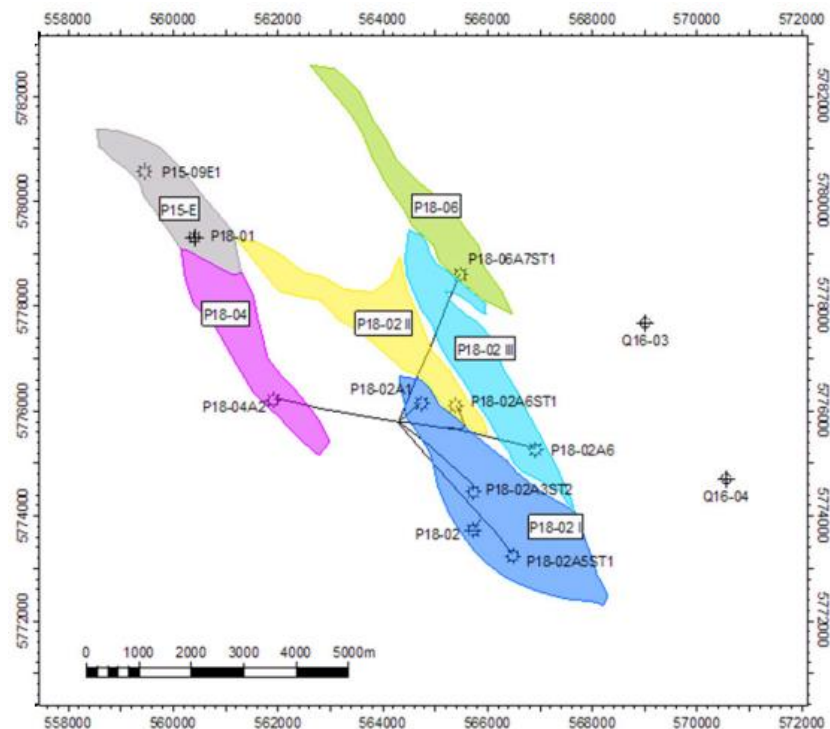


Figure 2 The compartmentalisation of the P18-A block (after Paginer *et al.* (2011), the CATO-2 project).

2.1.1 Structural history

The deposition and deformation of the P18-A block was strongly controlled by a sequence of rift pluses that started during the Late Triassic period (Arts *et al.*, 2012). Prior to the rifting events, sedimentation initially included the lacustrine sediments, followed by sandy fluvial and Aeolian successions that constitute the Main Buntsandstein Subgroup. During the active rifting period, several rift pulses broke up the basin into a number of NW-SE trending compartments bounded by faults (De Jager, 2007). Figure 2 illustrates the compartments that resulted from the rifting events in the P18-A block.

2.1.2 Reservoir geology

The structures containing the depleted gas reservoirs are bounded by the faults in a horst and graben configuration, with a sinistral strike-slip component. The reservoir rocks are broadly divided into three formations formed by the cyclic alternation of arkosic sandstones and clayey siltstones of approximately 200m in thickness (Arts *et al.*, 2012).

The Volpriehausen formation at the bottom part of the reservoir is mainly fluvial, but also contains some aeolian sediments. It consists of braided river deposits interbedded with subordinate flood-plain and crevasse-splay and locally dune deposits (Ames and Farfan, 1996).

The overlying Detfurth formation comprises mainly of aeolian sediments (dunes), with some fluvial deposits (Ames and Farfan, 1996). It is generally marked by low gamma-ray values owing to the presence of quartz-cementation (Geluk *et al.*, 1996). The upper part of the formation is distinctly separated from the lower part by a well-correlatable interval of relatively higher gamma-ray values and a single coarsening-upward sequence.

The Hardeggen formation is the youngest part of the Main Buntsandstein Subgroup. It mainly consists of aeolian deposits overlain by the Solling sandstone member at the top part of the

reservoir, which is characterised by an increase in the gamma-ray values compared to the underlying Detfurth formation.

2.2 P18-A reservoir model

2.2.1 Structural and geological model

A field-scale reservoir model of the P18-A block was made available by TNO in the MiReCOL project model database. The model was previously developed and history matched using gas production data within the Dutch CATO-2 research program. The model grid spans an area of approximately 20.5km×7.5km and includes several faults whose structural characteristics result in variable horizontal transmissibility ranging from sealing to non-sealing nature.

The grid represents the Main Buntsandstein reservoir subdivided into four zones, namely (from bottom to top): (1) the Volpriehausen formation with an average thickness of 115m and resolution of 50m×50m×115m; (2) the lower Detfurth formation with an average thickness of 22m and resolution of 50m×50m×22m; (3) the upper Detfurth formation with an average thickness of 48m and resolution of 50m×50m×48m; and (4) the Hardegsen formation with an average thickness of 30m and resolution of 50m×50m×30m. The depth of the model ranges between 2,850m and 4,500m. Figure 3 illustrates the structural model of the depleted gas fields in the P18-A block and well locations previously used for gas production.

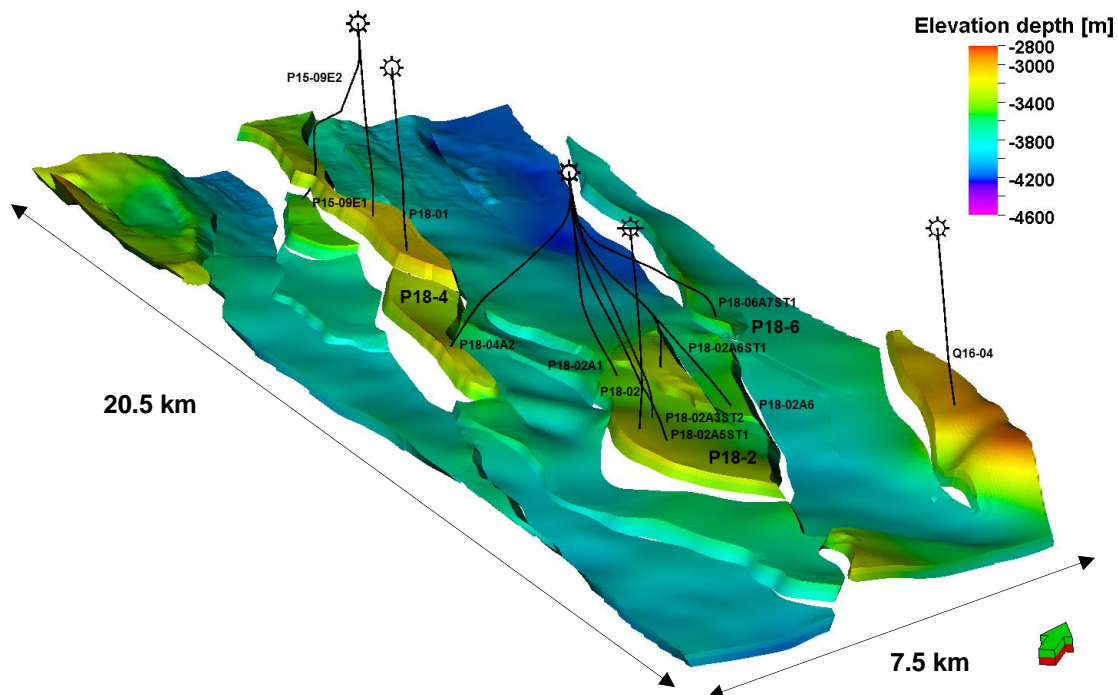


Figure 3 The structural model of the P18-A block and well locations.

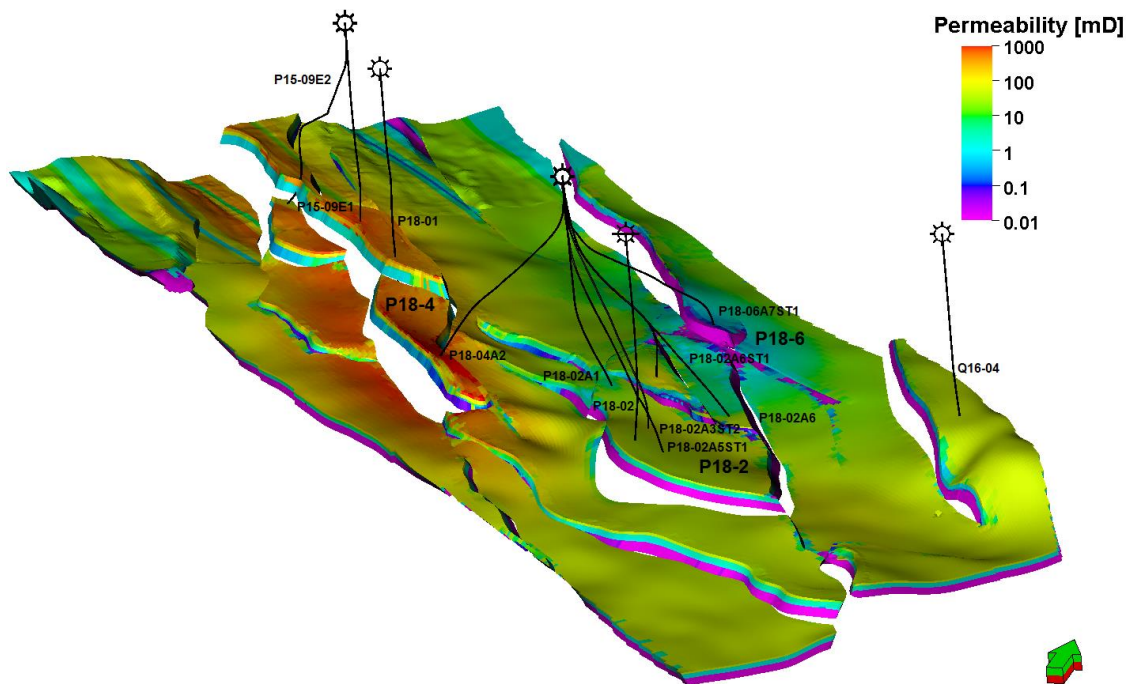


Figure 4 The horizontal permeability distribution of the P18-A block.

The MiReCOL database also includes the petrophysical property attributions for porosity, permeability and net-to-gross ratio that were generated by TNO from the information available in the well logs using the block kriging technique. Figure 4 illustrates the horizontal permeability distribution as an example. In addition, Table 1 summarises the petrophysical properties for different reservoir zones in the model.

Table 1 The summary of petrophysical properties in the model.

Reservoir zones	Porosity				Horizontal Permeability (mD)*				NTG			
	min	mean	max	st.dev	min	mean	max	st.dev	min	mean	max	st.dev
Hardeggen	0.01	0.08	0.18	0.03	10 ⁻⁴	130	1,977	206	0.01	0.96	1	0.1
Upper Detfurth	0.01	0.05	0.13	0.02	10 ⁻⁴	34	751	93	0.01	0.77	1	0.3
Lower Detfurth	0.01	0.05	0.11	0.02	10 ⁻⁵	24	1,133	97	0.01	0.83	1	0.3
Volpriehausen	0.01	0.03	0.11	0.01	10 ⁻⁵	0.16	307	1.8	0.01	0.25	1	0.3

* Vertical permeability = 0.1 × Horizontal permeability (Arts *et al.*, 2010)

2.2.2 Dynamic properties of the reservoir model

The initialisation for CO₂ injection and brine production simulations performed in this study is based on the depletion condition of the fields. The pressure in the fields of the P18-A block during the post-production period in 2015 was estimated to be in the range of 25-30 bars (Arts *et al.*, 2012; Tambach *et al.*, 2015). Previous simulation studies have also estimated that the dynamic capacity for CO₂ storage is 30.4Mt, 8.1Mt and 0.6Mt for the P18-2, P18-4 and P18-6 fields respectively, assuming a maximum allowable pressure limit of 350 bars according to the pre-production field conditions (Paginer *et al.*, 2011). The reservoir temperature was set to be constant at 120°C.

3 CO₂ FLOW DIVERSION AND PRESSURE MANAGEMENT IN THE RESERVOIR WITH BRINE WITHDRAWAL

A dynamic model for the simulation of CO₂ flow diversion with brine withdrawal was set up in Schlumberger’s Eclipse 300 (E300) software using the static geological model and the dynamic reservoir parameters described in the previous section. It is based on the compositional option for simulating CO₂ storage in depleted reservoirs, enabled by the CO2SOL option, wherein CO₂ can be present in three phases (Schlumberger, 2014). The modelling broadly comprise of three stages: CO₂ injection; termination of injection when plume migration beyond the field boundary (due to overfilling of the reservoir) is detected; and flow diversion of the plume with brine production.

The P18-2 field was selected for the purposes of the study in this report since it is a relatively larger field in comparison to P18-4 and P18-6 (see Figure 2). As illustrated in Figure 5, it is subdivided into three compartments, namely P18-2 (1), P18-2 (2) and P18-2 (3), that are penetrated by six wells used for gas production.

3.1 CO₂ injection: plume migration and pressure analyses

Since the current study deals with a compartmentalised field model, it was deemed necessary to initially investigate the maximum possible CO₂ injection rates that could be implemented for each of the three compartments, the migration of the plume in the reservoir, and the pressure communication amongst the compartments, including the far-field region which lies beyond the boundary of the P18-2 field (see Figure 5). Suitable injection rates were thus chosen in order to maximise their respective dynamic capacities.

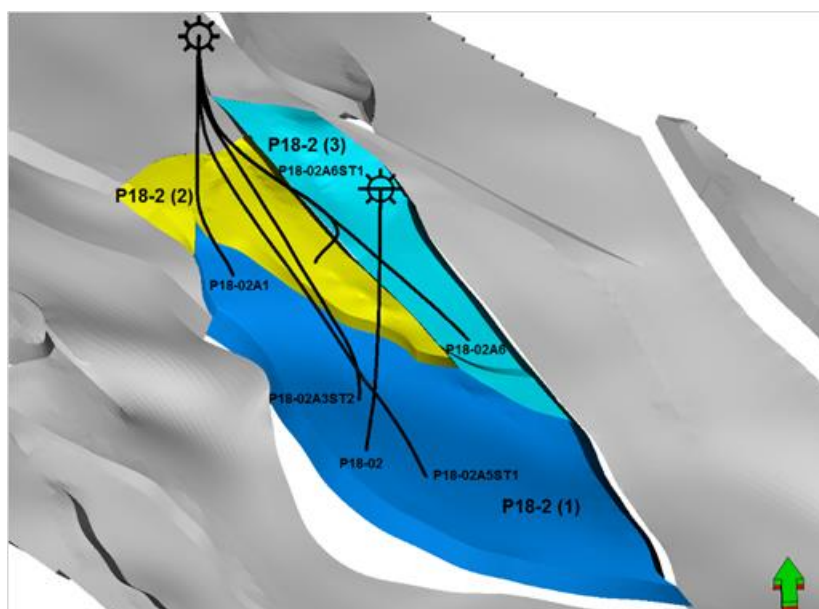


Figure 5 The P18-2 field compartments and well locations.

The migration of the plume in the reservoir was observed by visualising the gas saturation distribution and noting the fractions of the cumulative mass of injected CO₂ available in each of the compartments and the far-field region during the simulation period of 30 years.

The pressure in the compartments were also monitored during the simulation period in order to check if it ranges within the fracture pressure limit, which is assumed as $1.5 \times$ initial reservoir pressure, prior to gas production (=350 bars).

3.1.1 *Compartment P18-2 (1)*

The simulations for CO₂ injection in the 18-2 (1) compartment were carried out using the well P18-02. Multiple injection rates were assumed between 0-1Mt/year. The cumulative amount of CO₂ injected and the corresponding pressure build-up in the compartment were noted. The highest possible rate of injection in the compartment is 0.66Mt/year (Figure 6) while ensuring that the pressure is being maintained within the fracture pressure limit of 525 bars during the simulation period (Figure 7). Hence, the cumulative amount of CO₂ injected is 19.8Mt in 30 years.

Figure 8 illustrates the plume migration in and outside the P18-2(1) compartment during CO₂ injection at 0.66Mt/year.

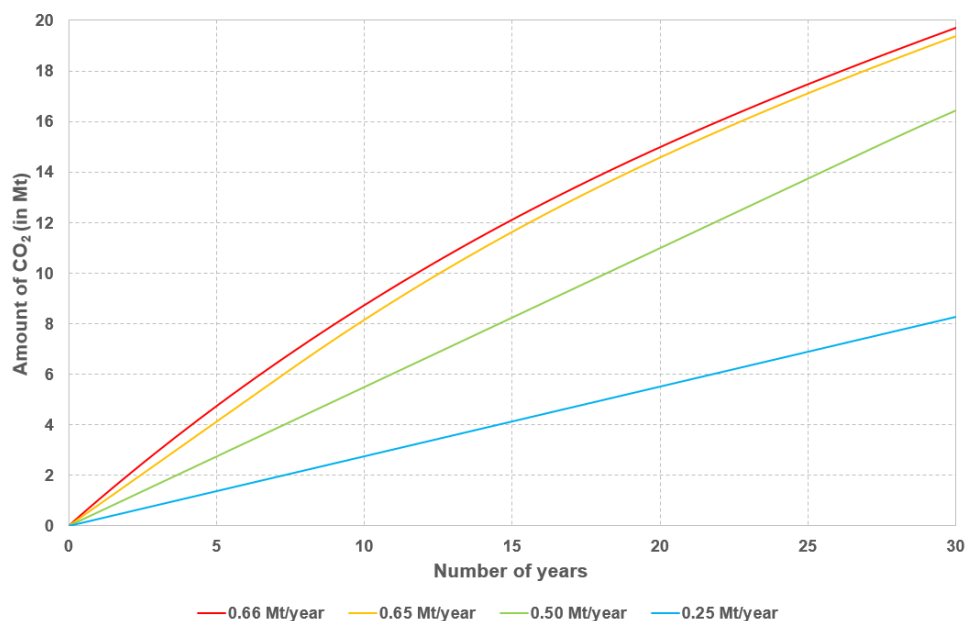


Figure 6 Cumulative amount of CO₂ injected into the P18-2 (1) compartment for different injection rates.

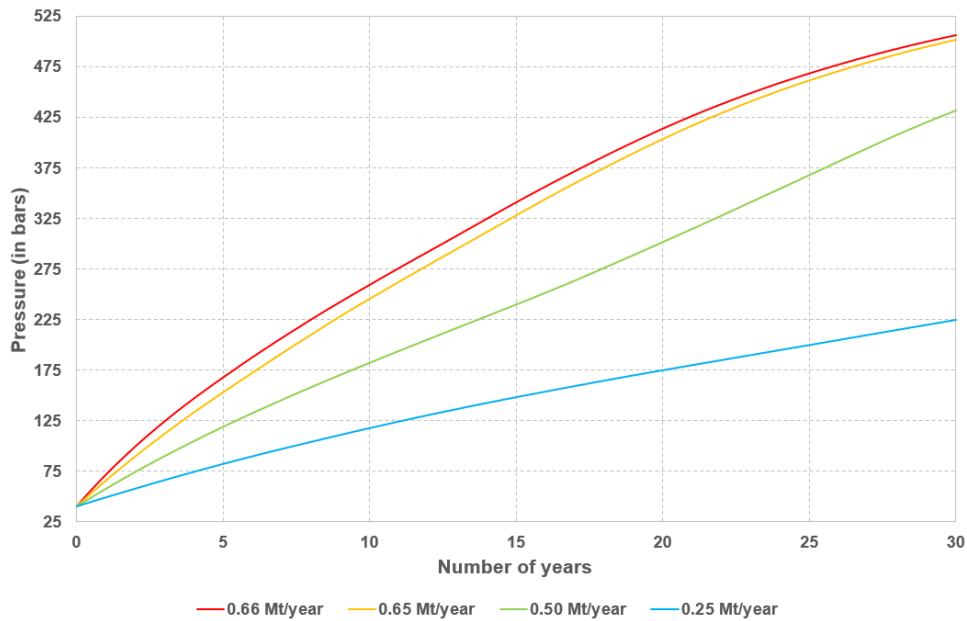


Figure 7 Pressure development in the P18-2 (1) compartment for different injection rates.

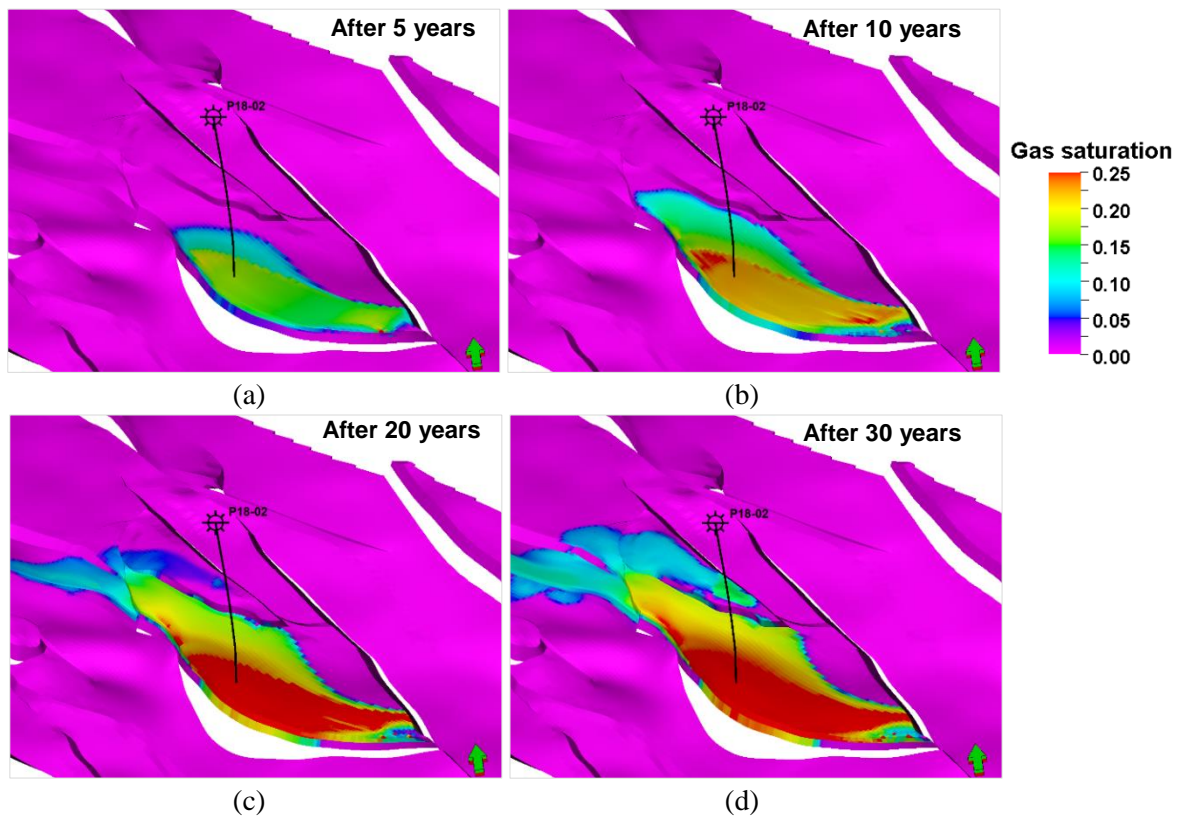


Figure 8 The estimated CO₂ plume distribution and its evolution in and outside the P18-2(1) compartment during CO₂ injection at 0.66Mt/year: (a) after 5 years; (b) after 10 years; (c) after 20 years; (d) after 30 years.

The fractions of the plume migrating outside the compartment, as illustrated in Figure 9, is related to the reservoir permeability, horizontal fault transmissibility and pressure build-up in the neighbouring compartments. For example, the highest fractional amount of plume migration occurring outside the P18-2 field, which corresponds to 1.19Mt CO₂, is caused by the relatively higher dynamic pressure gradient created between the compartments during injection (Figure 10).

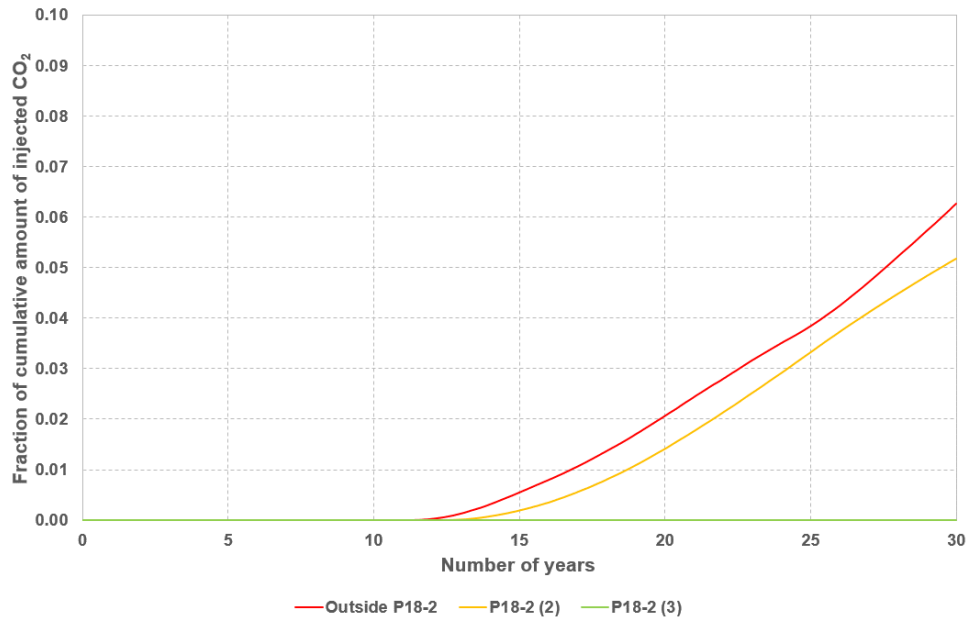


Figure 9 Plume migration outside the P18-2 (1) compartment during CO₂ injection at 0.66Mt/year, expressed as the fraction of the cumulative amount of CO₂.

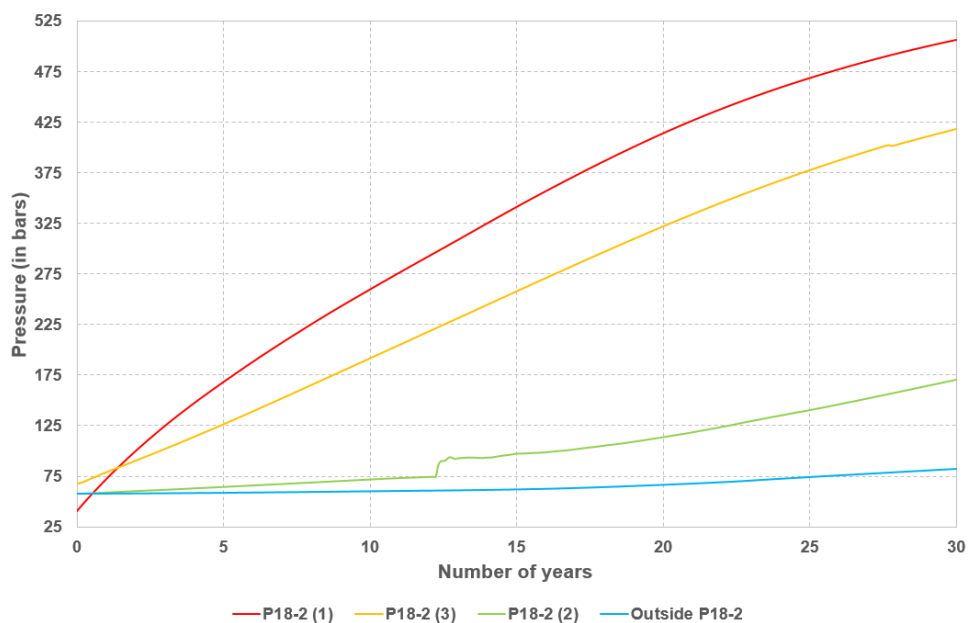


Figure 10 Pressure development in different compartments during CO₂ injection at 0.66Mt/year.

3.1.2 Compartment P18-2 (2)

The simulations for CO₂ injection in the 18-2 (2) compartment were carried out using the well P18-02A6ST1. Multiple injection rates were assumed between 0-1Mt/year. The cumulative amount of CO₂ injected and the corresponding pressure build-up in the compartment were noted.

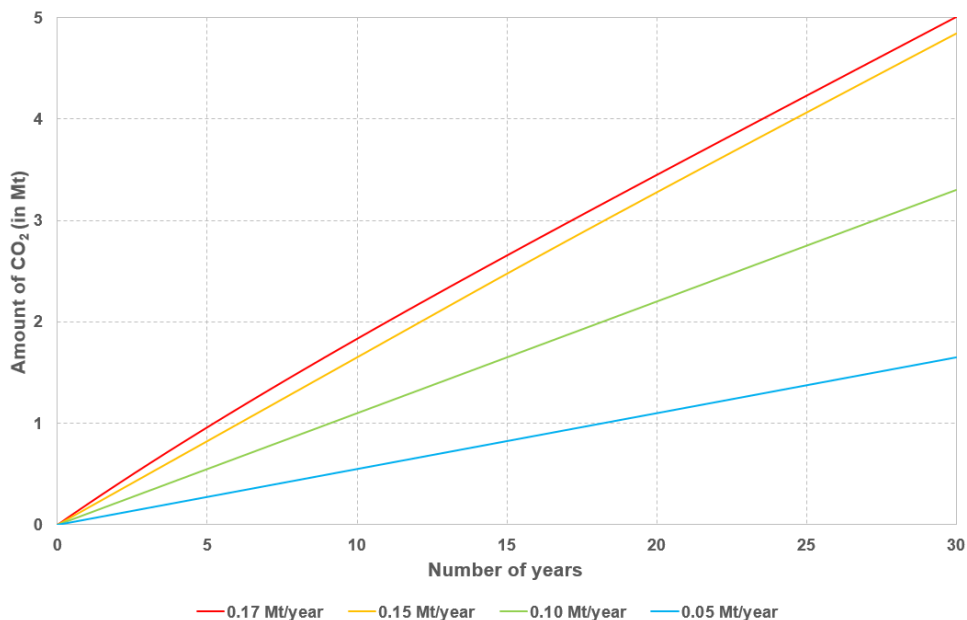


Figure 11 Cumulative amount of CO₂ injected into the P18-2 (2) compartment for different injection rates.

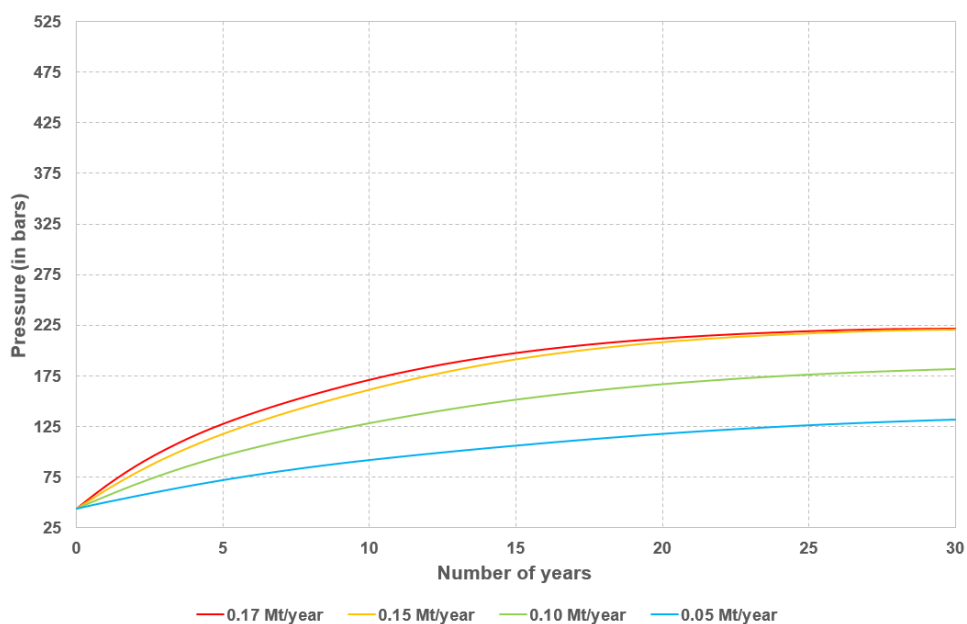


Figure 12 Pressure development in the P18-2 (2) compartment for different injection rates.

The simulations suggest that the highest possible rate of injection in the compartment is 0.17Mt/year (Figure 11). The pressure increase is also well within the fracture pressure limit during the simulation period (Figure 12). Hence, the cumulative amount of CO₂ injected is 5.1Mt in 30 years.

Figure 13 illustrates the plume migration in and outside the P18-2(2) compartment during CO₂ injection at 0.17Mt/year.

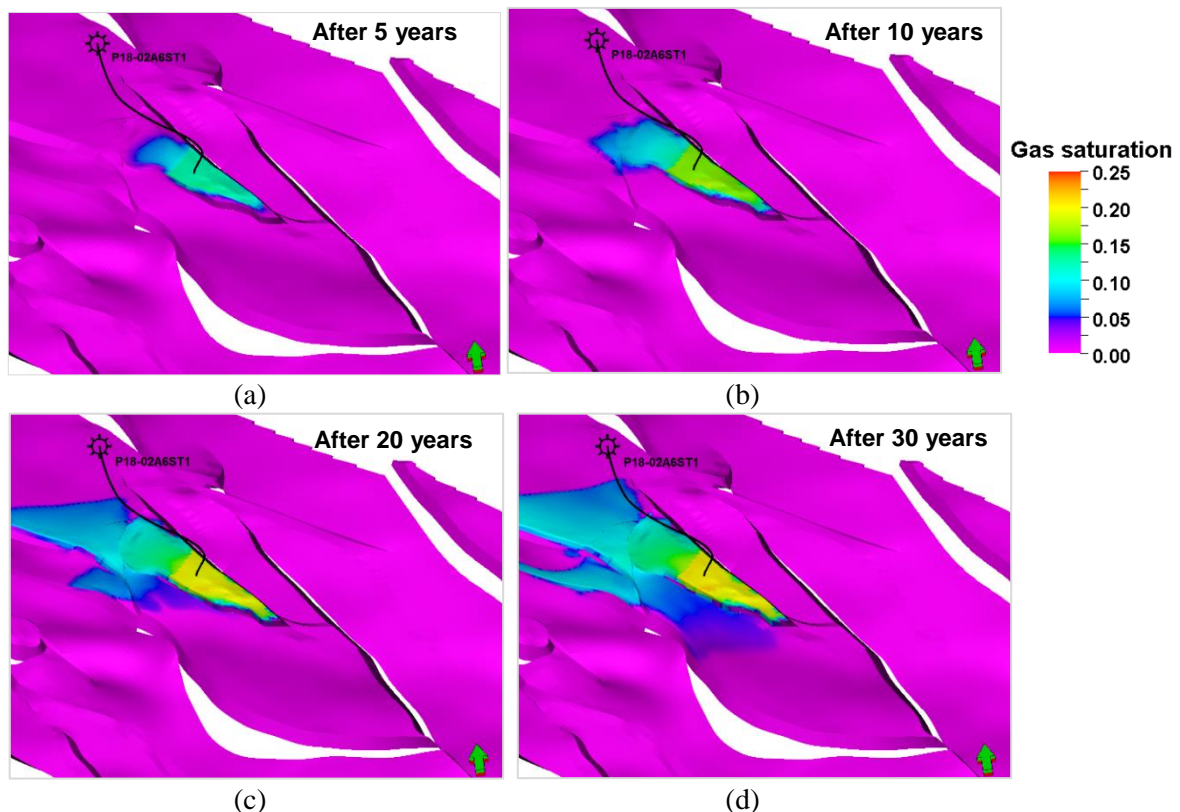


Figure 13 The estimated CO₂ plume distribution and its evolution in and outside the P18-2 (2) compartment during CO₂ injection at 0.17Mt/year : (a) after 5 years; (b) after 10 years; (c) after 20 years; (d) after 30 years.

The highest fractional amount of plume migration of 1.33Mt CO₂ occurs outside the P18-2 field. Correspondingly, a large fraction of 26% indicated in Figure 14 suggests that owing to its smaller size, the P18-2 (2) compartment is able to contain a lesser amount of CO₂ at the end of the simulation period (see Figure 13d) when compared to CO₂ injection in the P18-2 (1) compartment described previously.

In addition, the pressure development in various compartments as illustrated in Figure 15 suggests that the pressure gradient is largely isotropic in all directions (towards the P18-2 (1) and P18-2 (3) compartments, and outside the P18-2 field). Hence, when injection occurs in the P18-2 (2) compartment, there is a preferential migration of the plume outside the P18-2 field which is attributed to relatively higher horizontal transmissibility across the relevant faults.

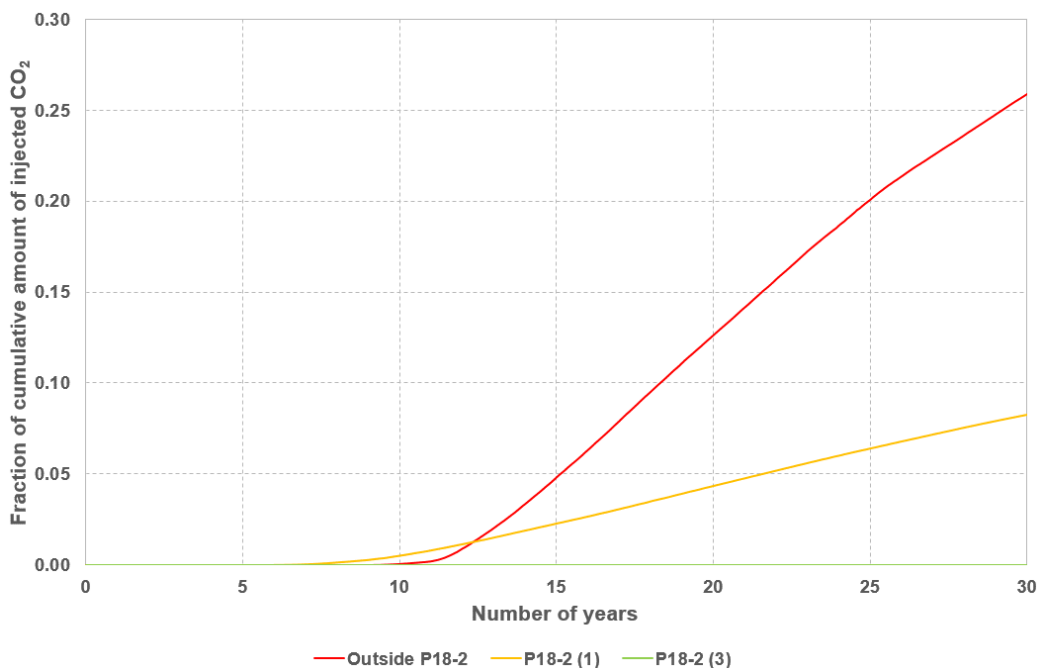


Figure 14 Plume migration outside the P18-2 (2) compartment during CO₂ injection at 0.17Mt/year, expressed as the fraction of the cumulative amount of CO₂.

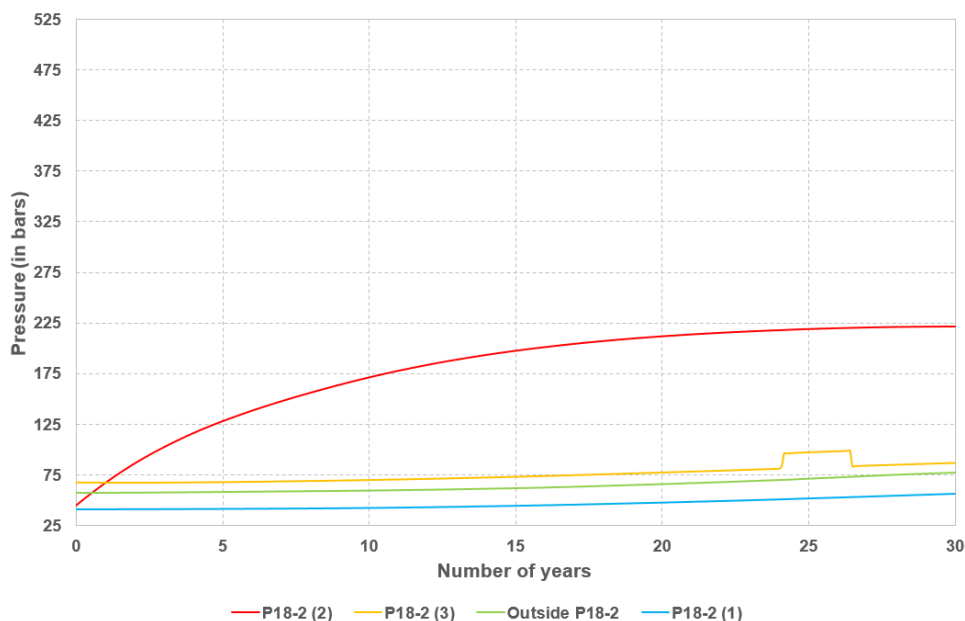


Figure 15 Pressure development in different compartments during CO₂ injection at 0.17Mt/year.

3.1.3 *Compartment P18-2 (3)*

The simulations for CO₂ injection in the 18-2 (3) compartment were carried out using the well P18-02A6. Multiple injection rates were assumed between 0-1Mt/year. The cumulative amount of CO₂ injected and the corresponding pressure build-up in the compartment were noted.

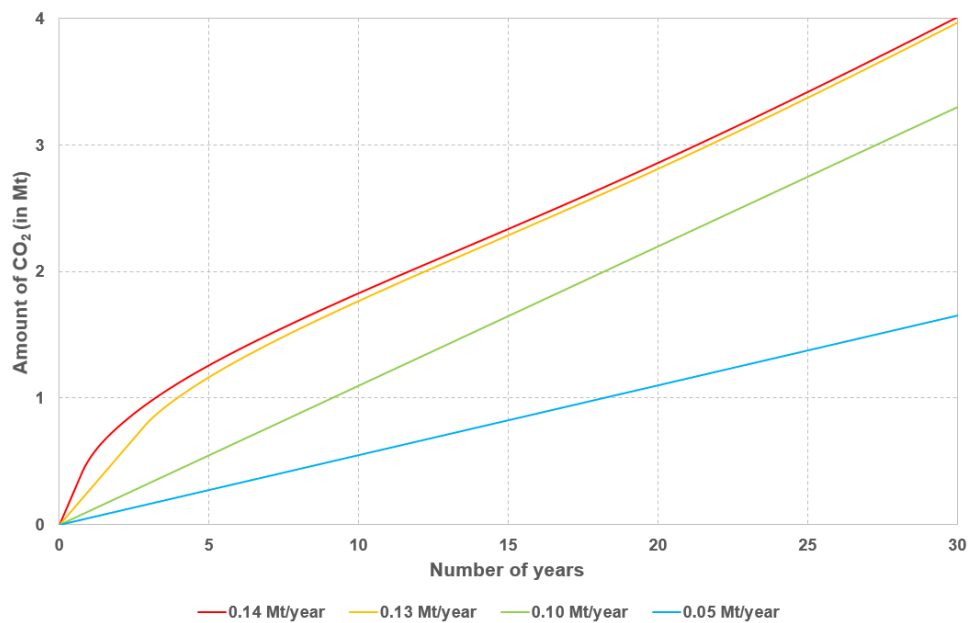


Figure 16 Cumulative amount of CO₂ injected into the P18-2 (3) compartment for different injection rates.

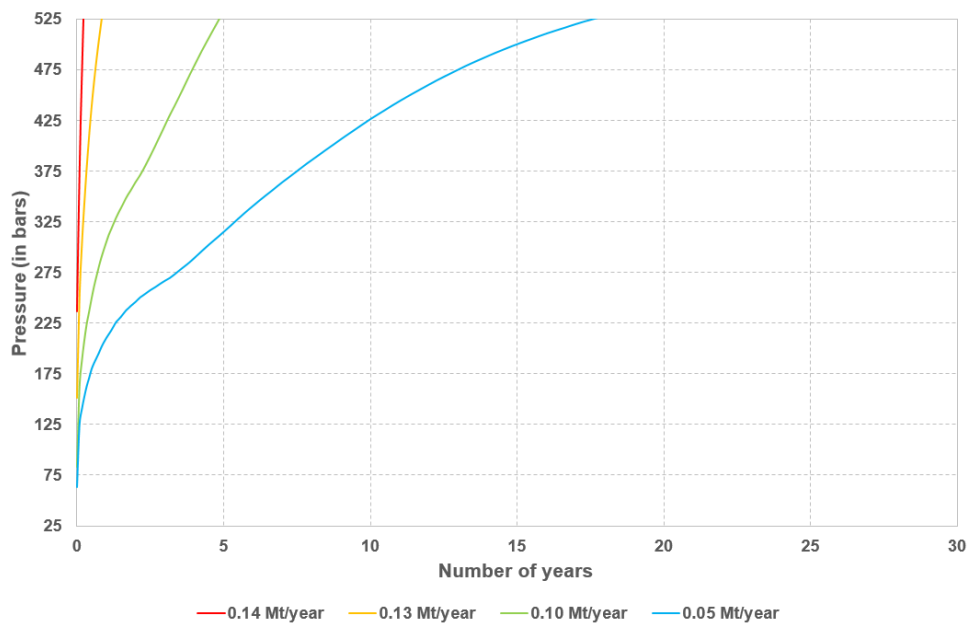


Figure 17 Pressure development in the P18-2 (3) compartment for different injection rates.

The highest possible rate of injection in the compartment is found to be 0.05Mt/year (Figure 16). This is unlike the previous scenarios (injection in the P18-2 (1) and P18-2 (2) compartments) because Figure 17 suggests that, for the injection rates that were simulated, the pressure build-up in the P18-2 (3) compartment exceeds the fracture pressure limit during the simulation period. This is largely due to relatively lower horizontal transmissibility of the bounding faults and lower reservoir permeability in the compartment. Hence, the highest cumulative amount of CO₂ achieved is 0.875Mt in 17.5 years, as a trade-off when injected at a lower injection rate of 0.05Mt/year. The simulation results also suggest that injection at higher rates ideally requires

termination within five years of operation (Figure 17), although for the sake of the discussion of the results, all simulations were run for 30 years (see Figure 16).

Figure 18 illustrates the plume migration in and outside the P18-2(3) compartment during CO₂ injection at 0.05Mt/year.

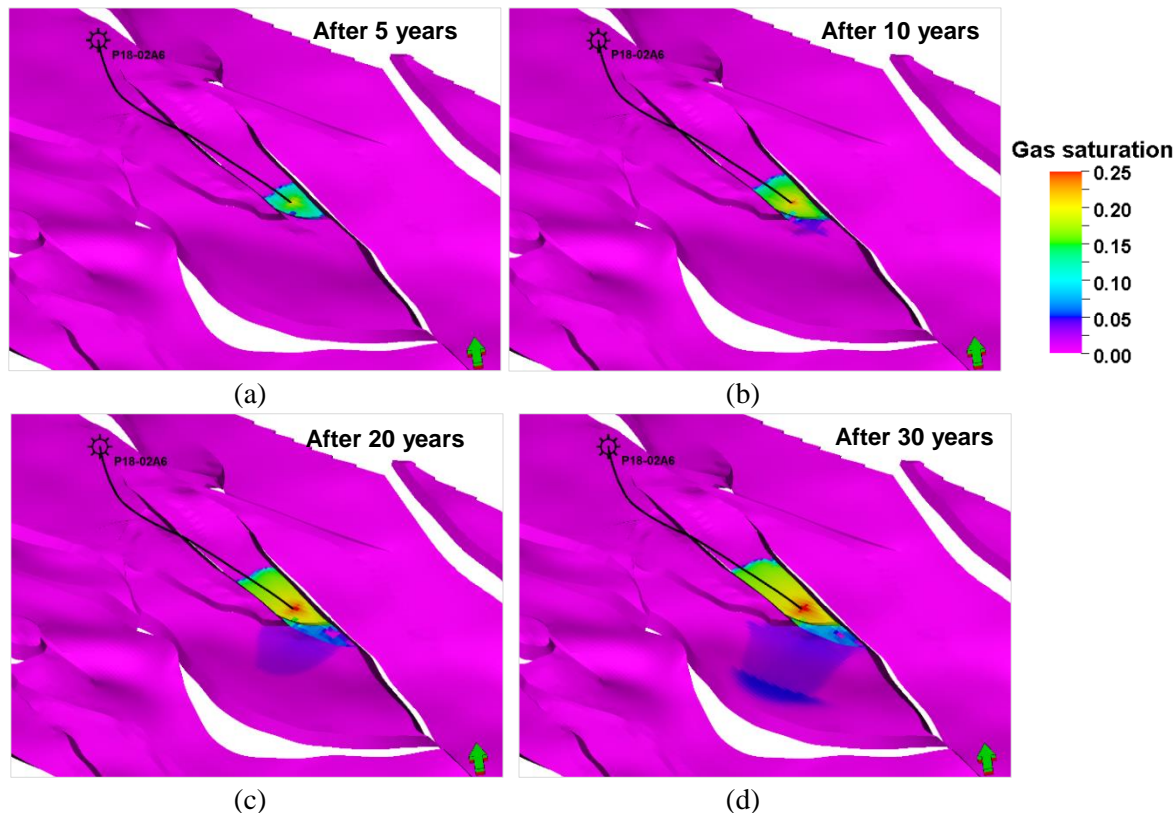


Figure 18 The estimated CO₂ plume distribution and its evolution in and outside the P18-2 (3) compartment during CO₂ injection at 0.05Mt/year: (a) after 5 years; (b) after 10 years; (c) after 20 years; (d) after 30 years.

The highest fractional amount of plume migration of 0.375Mt CO₂ occurs in the P18-2 (1) compartment. This plume migration is desirable since it shows that CO₂ storage occurs within the limits of the P18-2 field, as illustrated in Figure 19.

On the contrary, the pressure development results in Figure 20 clearly suggests that the available storage capacity would be underutilised if the injection needs to be stopped after 17.5 years of operation (an example for plume distribution is shown for 20 years in Figure 18c), as opposed to the planned period of 30 years. Moreover, the reservoir topography suggests that the P18-2 (3) is a low-lying compartment when compared to P18-2 (1), and hence buoyancy would also enhance the dynamic storage capacity during injection, provided suitable measures are taken to maintain the compartment pressure within the fracture pressure limit. In this context, brine production has been investigated as an option for pressure management, which is to be discussed in the following sections, although re-starting CO₂ injection after pressure management is not in the scope of this study.

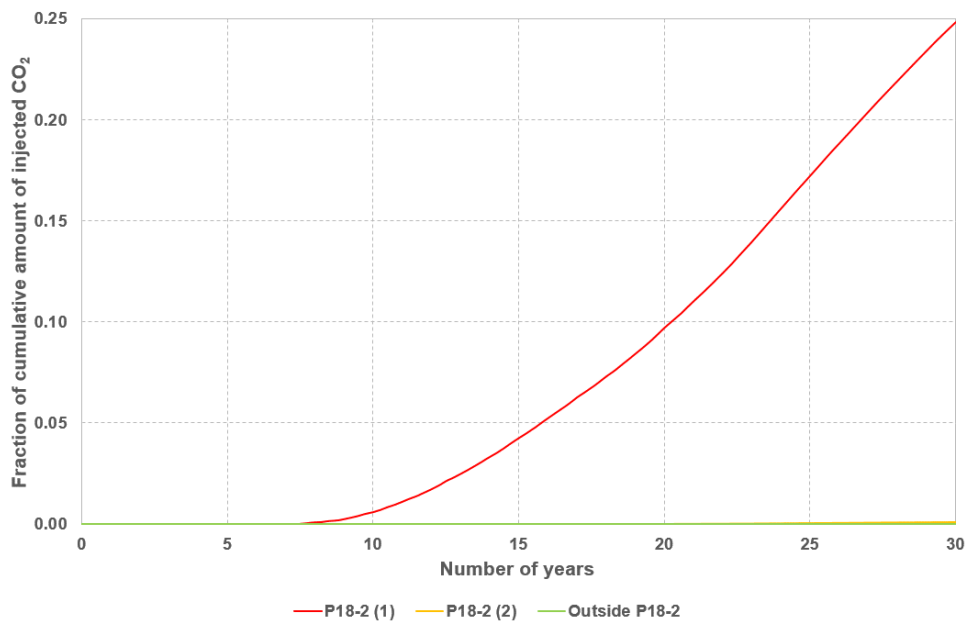


Figure 19 Plume migration outside the P18-2 (3) compartment during CO₂ injection at 0.05Mt/year, expressed as the fraction of the cumulative amount of CO₂.

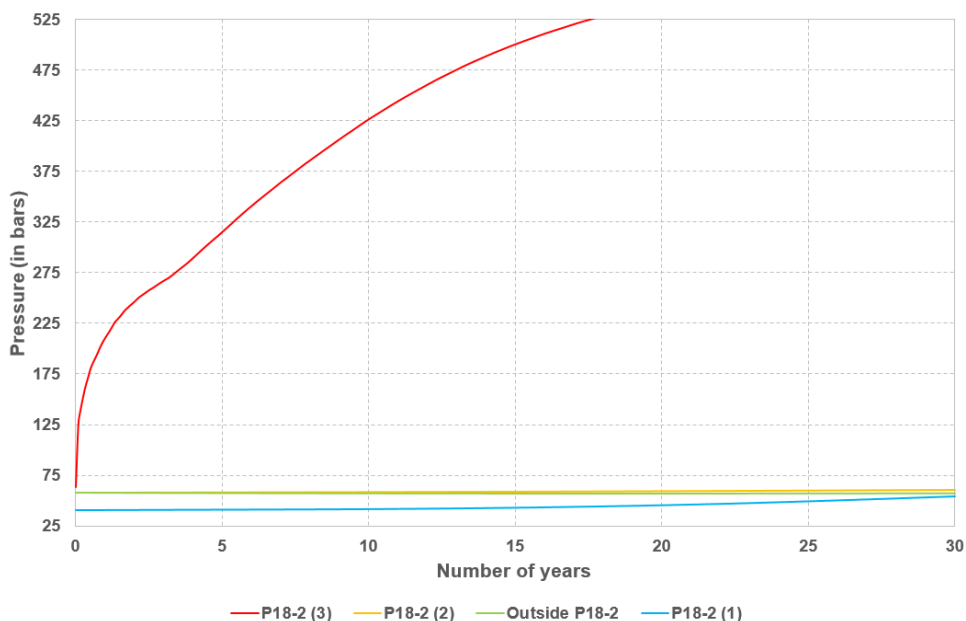


Figure 20 Pressure development in different compartments during CO₂ injection at 0.05Mt/year.

3.2 Relaxation of the reservoir

Based on the discussion of the results obtained in the previous sections, two stopping criteria for CO₂ injection were thus assumed: (a) when the plume migrates beyond the boundary of P18-2 field (all three compartments taken together) during CO₂ injection in the P18-2 (1) and P18-2 (2) compartments; and (b) when the pressure in the P18-2 (3) compartment approaches the fracture pressure limit during injection.

3.2.1 Compartment P18-2 (1)

The simulation for CO₂ injection in the 18-2 (1) compartment was carried out at a rate of 0.66Mt/year using the well P18-02. It was observed that after 13 years of simulation, the plume migrates outside the P18-2 field. This corresponds to 5000 tonnes CO₂ in the far-field which was assumed as the lower detection limit (Benson, 2006). The injection was stopped and the reservoir was allowed to equilibrate during the remaining period of the simulation.

Figure 21a illustrates the plume distribution after 13 years, when the migration occurring outside the P18-2 field boundary was detected. The cumulative amount of CO₂ injected in the compartment is 8.58Mt.

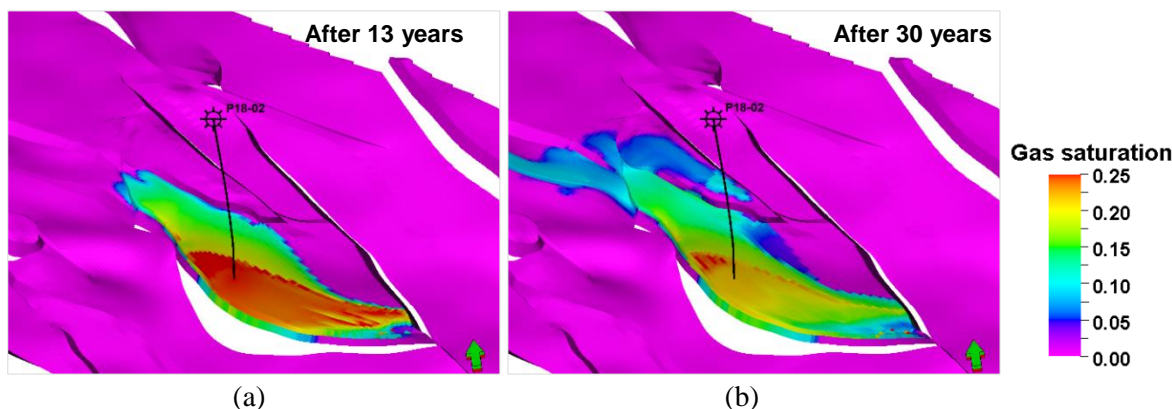


Figure 21 The estimated CO₂ plume distribution and its evolution in and outside the P18-2 (1) compartment: (a) after 13 years when the plume migrates outside the P18-2 field and CO₂ injection simulation was stopped; (b) after 30 years.

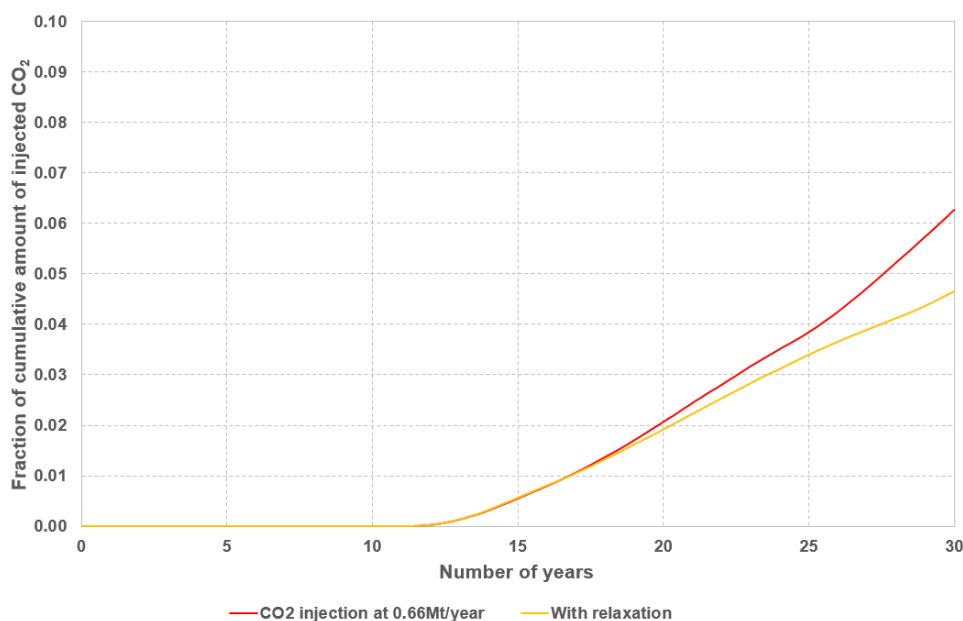


Figure 22. Comparison of plume migration outside the P18-2 field, expressed as the fraction of the cumulative amount of CO₂.

The fractional amount of CO₂ which migrates outside the field during the remaining period of equilibration (Figure 21b) corresponds to 0.39Mt CO₂, and it is smaller when compared to 1.19 Mt CO₂ if the injection were sustained for 30 years (Figure 22), as described previously.

Hence, by stopping CO₂ injection, it is estimated that approximately 23% reduction in plume migration beyond the field boundary was achieved per unit Mt of injected CO₂.

3.2.2 *Compartment P18-2 (2)*

The simulation for CO₂ injection in the 18-2 (2) compartment was carried out at a rate of 0.17Mt/year using the well P18-02A6ST1. It was observed that after 8 years of simulation, the plume migrates outside the P18-2 field, and thus the stopping criterion was applied thereafter. Figure 23a illustrates the plume distribution after 8 years, when the cumulative amount of CO₂ injected in the compartment is 1.36Mt.

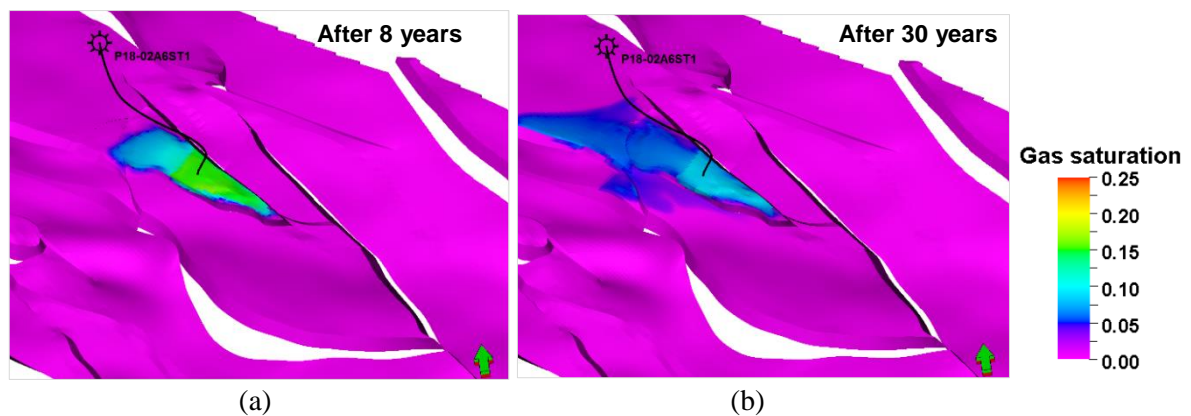


Figure 23 The estimated CO₂ plume distribution and its evolution in and outside the P18-2 (2) compartment: (a) after 8 years when the plume migrates outside the P18-2 field and CO₂ injection simulation was stopped; (b) after 30 years.

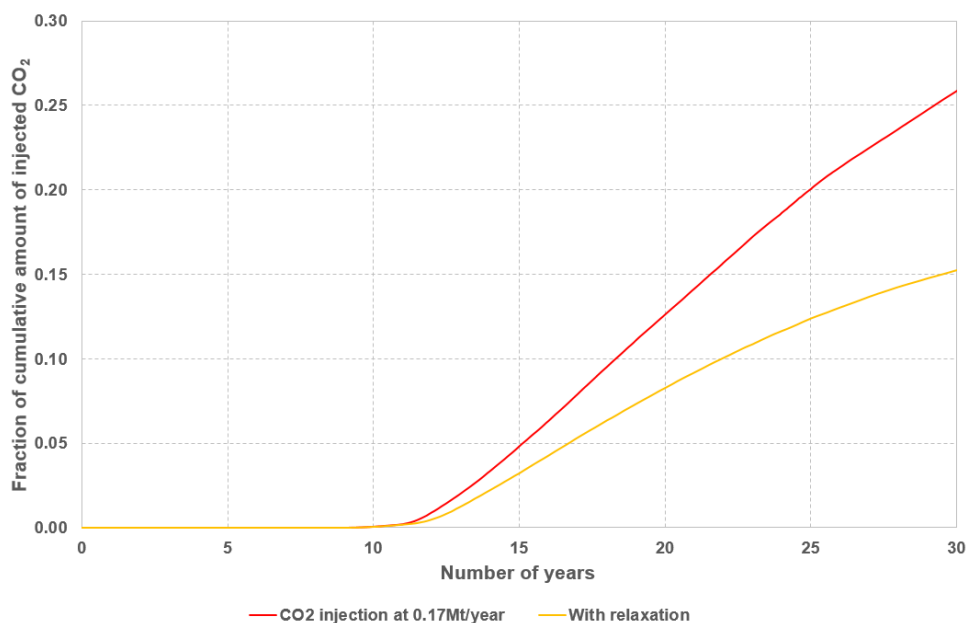


Figure 24. Comparison of plume migration outside the P18-2 field, expressed as the fraction of the cumulative amount of CO₂.

The fractional amount of CO₂ which migrates outside the field during the remaining period of equilibration (Figure 23b) corresponds to 0.2Mt CO₂, and it is smaller when compared to 1.33Mt CO₂ if the injection were sustained for 30 years (Figure 24), as described previously. Hence, by stopping CO₂ injection, it is estimated that approximately 42% reduction in plume migration beyond the field boundary was achieved per unit Mt of injected CO₂.

3.2.3 Compartment P18-2 (3)

The simulation for CO₂ injection in the 18-2 (3) compartment was carried out at a rate of 0.05Mt/year using the well P18-02A6. It was observed that after 17 years of simulation, the pressure in the compartment approaches the fracture pressure of 525 bars, and thus the stopping criterion was applied thereafter. Figure 25a illustrates the plume distribution after 17 years, when the cumulative amount of CO₂ injected in the compartment is 0.85Mt.

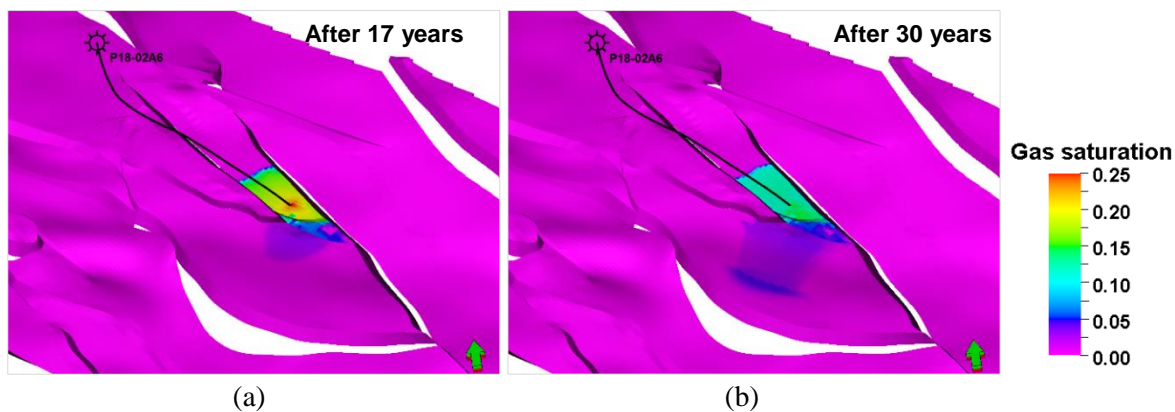


Figure 25 The estimated CO₂ plume distribution and its evolution in and outside the P18-2 (3) compartment: (a) after 17 years when the pressure in the compartment approaches the fracture pressure (525 bars) and CO₂ injection simulation was stopped; (b) after 30 years.

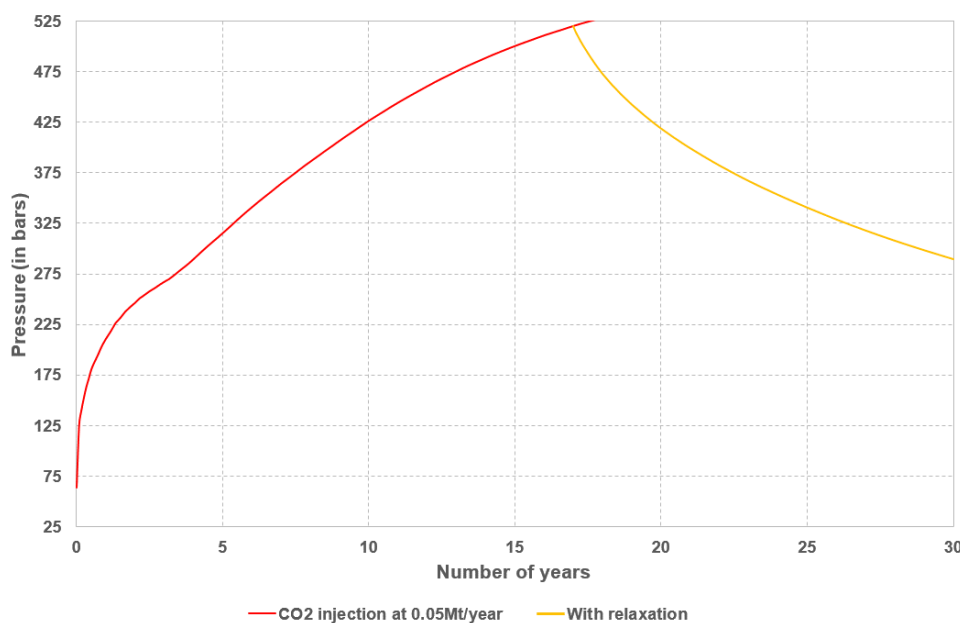


Figure 26 Pressure development in the P18-2 (3) compartment during CO₂ injection at 0.05Mt/year (for 17 years) and after the relaxation criterion is applied (for 13 years).

A pressure reduction of approximately 45% was achieved as a result of pressure equilibration to 290 bars (Figure 26), while the plume is retained within the P18-2 field (Figure 25b). It thus provides the necessary and sufficient condition to re-start CO₂ injection after 30 years. However, this would fall under a separate study on the maximisation of reservoir capacity utilisation, which is currently outside the scope of the current objectives.

3.3 Brine withdrawal

Brine withdrawal simulations were carried out for each scenario by making similar assumptions for the injection stopping criteria as discussed for reservoir relaxation. The brine production well layouts were chosen in such a way that there is a minimum risk of CO₂ breakthrough during the simulation period is expected. The issues related to CO₂ breakthrough would fall under a separate study on risk assessment, which is currently outside the scope of the current objectives.

3.3.1 *Compartment P18-2 (1)*

The simulation for CO₂ injection in the 18-2 (1) compartment was carried out at a rate of 0.66Mt/year using the well P18-02 (Figure 27a). When the plume migration occurs outside the P18-2 field after 13 years of simulation, CO₂ injection was stopped and brine production at the vertical well P18-02A6 (Figure 27b) was started simultaneously.

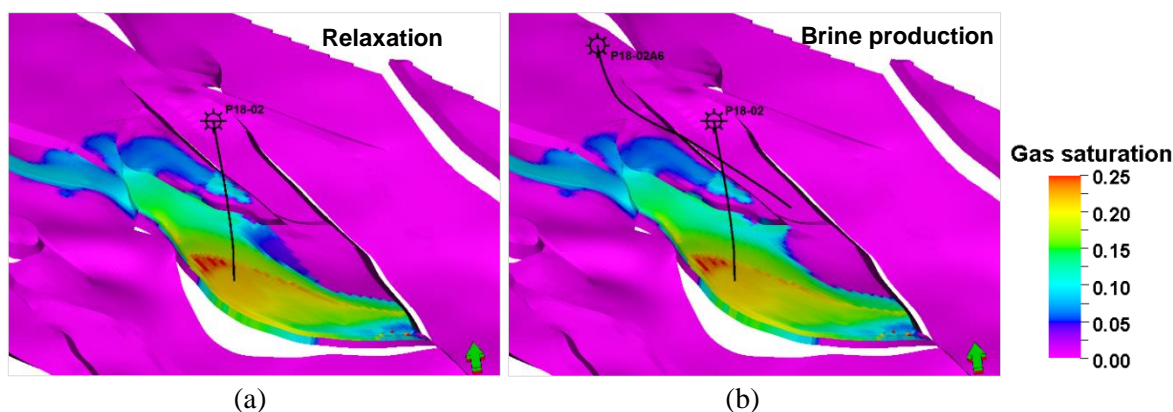


Figure 27 Comparison of the estimated CO₂ plume distribution in and outside the P18-2 (1) compartment after 30 years: (a) relaxation; (b) brine production.

Figure 27 illustrates the plume distribution at the end of the simulation period. The cumulative amount of CO₂ injected in the compartment is 8.58Mt. The fractional amount of CO₂ which migrates outside the field with brine production (Figure 28) corresponds to 0.34Mt CO₂. It is estimated that approximately 33% reduction in plume migration beyond the field boundary was achieved per unit Mt of injected CO₂ when brine production was applied.

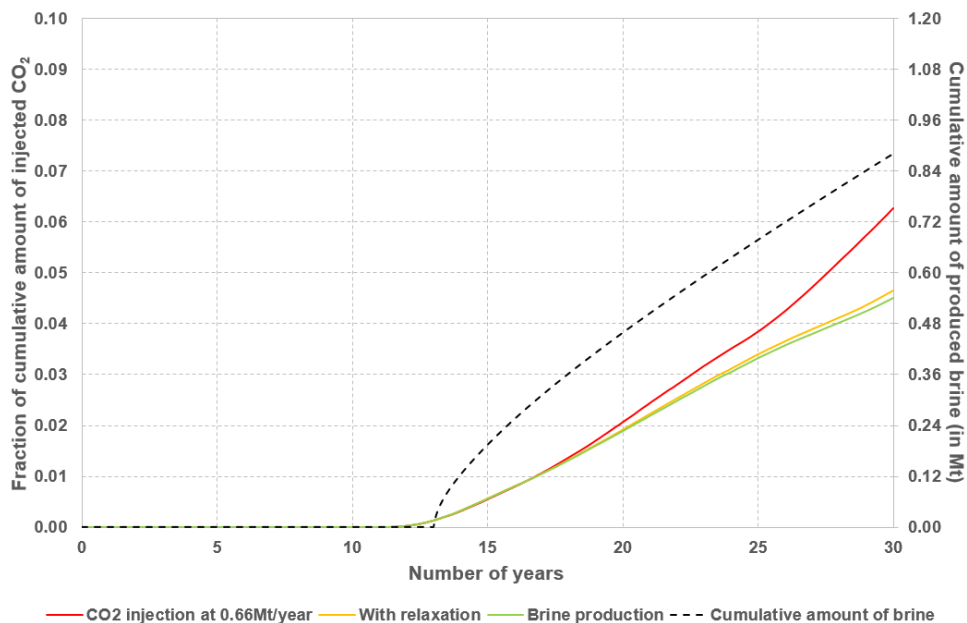


Figure 28 Comparison of plume migration outside the P18-2 field, expressed as the fraction of the cumulative amount of CO₂ and the cumulative amount of brine produced, represented on the secondary axis.

3.3.2 *Compartment P18-2 (2)*

The simulation for CO₂ injection in the 18-2 (2) compartment was carried out at a rate of 0.17Mt/year using the well P18-02A6ST1 (Figure 29a). When the plume migration occurs outside the P18-2 field after 8 years of simulation, CO₂ injection was stopped and brine production at four vertical wells, namely P18-02, P18-02A3ST2, P18-02A5ST1 and P18-02A6 (Figure 29b) was started simultaneously.

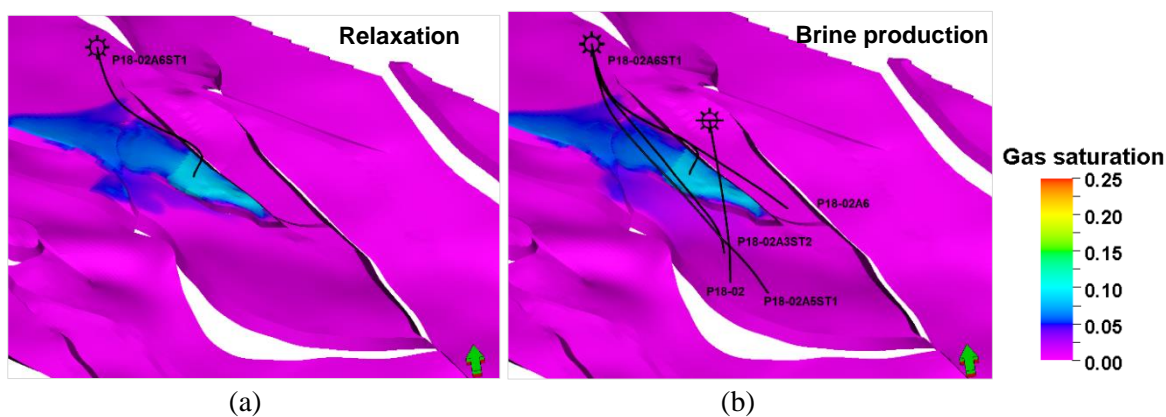


Figure 29 Comparison of the estimated CO₂ plume distribution in and outside the P18-2 (2) compartment after 30 years: (a) relaxation; (b) brine production.

Figure 29 illustrates the plume distribution at the end of the simulation period. The cumulative amount of CO₂ injected in the compartment is 1.36Mt. The fractional amount of CO₂ which migrates outside the field with brine production (Figure 30) corresponds to 0.19Mt CO₂. It is

estimated that approximately 46% reduction in plume migration beyond the field boundary was achieved per unit Mt of injected CO₂ when brine production was applied.

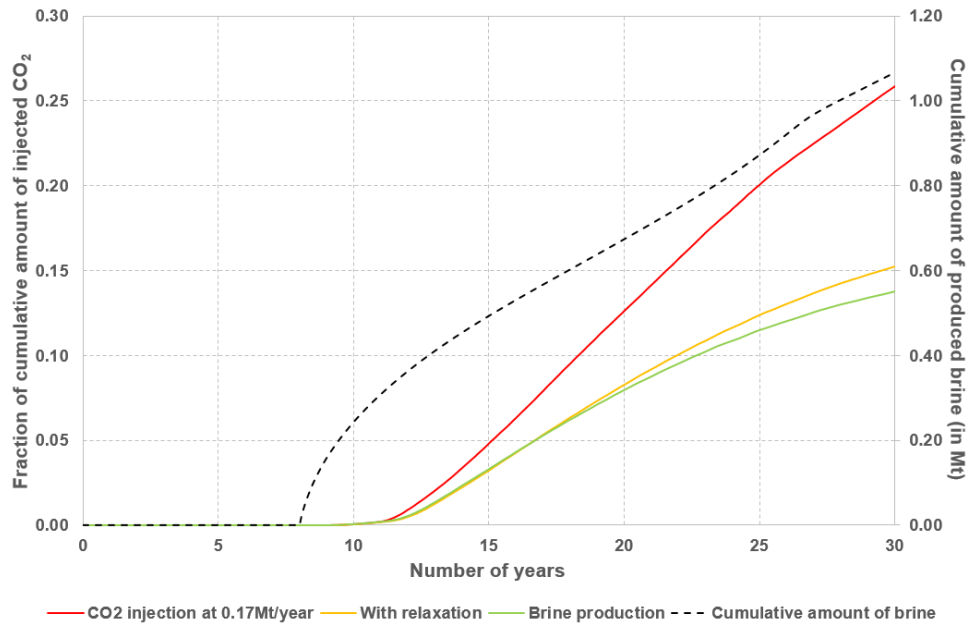


Figure 30 Comparison of plume migration outside the P18-2 field, expressed as the fraction of the cumulative amount of CO₂ and the cumulative amount of brine produced, represented on the secondary axis.

3.3.3 Compartment P18-2 (3)

The simulation for CO₂ injection in the 18-2 (3) compartment was carried out at a rate of 0.05Mt/year using the well P18-02A6 (Figure 31a). When the pressure in the compartment approaches the fracture pressure of 525 bars after 17 years of simulation, CO₂ injection was stopped. It was assumed that a horizontal well extension is drilled, essentially deeper (-3,640m) than the injection interval (-3,490m) to ensure no immediate CO₂ breakthrough occurs.

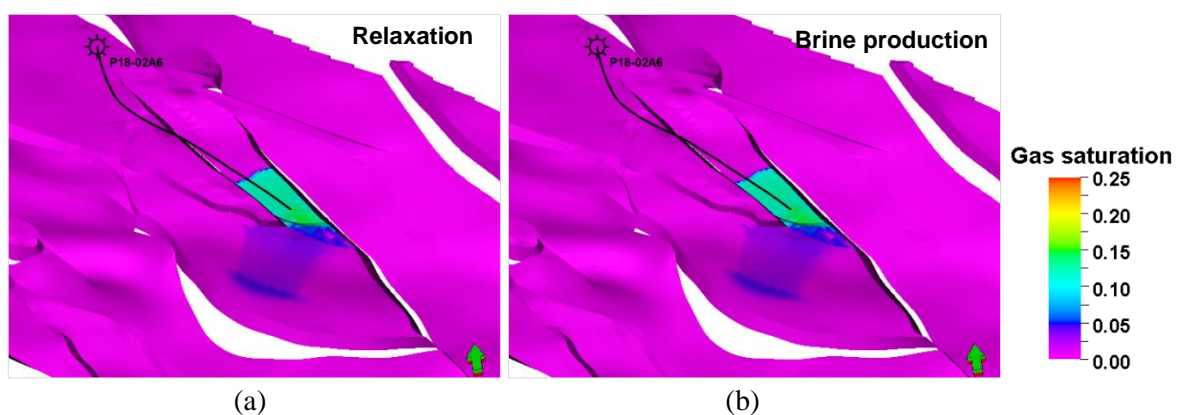


Figure 31 Comparison of the estimated CO₂ plume distribution in and outside the P18-2 (3) compartment after 30 years: (a) relaxation; (b) brine production.

Prior to brine production, it was also assumed that drilling a horizontal well extension of 250m in the reservoir would require one year. Figure 31 illustrates the plume distribution at the end of

the simulation period indicating that the plume is retained within the P18-2 field at the end of the simulation period. Figure 32 illustrates that a significant pressure reduction of approximately 84% was achieved as a result of brine production (to 85 bars).

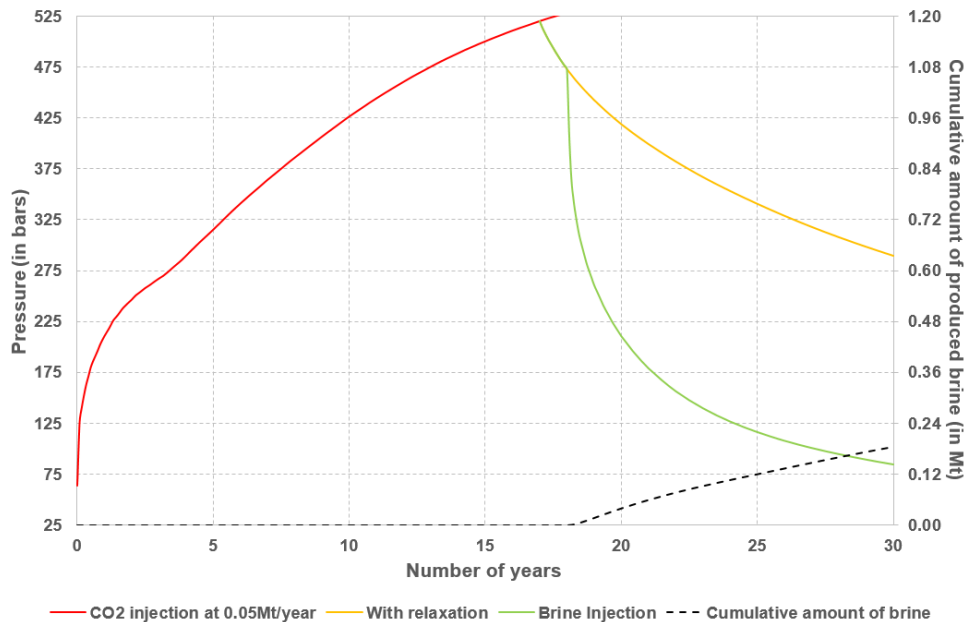


Figure 32 Comparison of pressure development in the P18-2 (3) compartment and the cumulative amount of brine produced, represented on the secondary axis.

3.3.4 Summary of the key performance indicators

Table 2 lists a summary of the KPIs determined for each of the scenarios for brine production assessed in this study.

Table 2 The summary of KPIs.

KPI	Scenario 1: CO ₂ injection in 18-2 (1)	Scenario 2: CO ₂ injection in 18-2 (2)	Scenario 3: CO ₂ injection in 18-2 (3)
Well Layout	1 vertical well	4 vertical wells	1 horizontal well
Volume of Brine extracted (in Mt)	0.9 (see Figure 28)	1.1 (see Figure 30)	0.2 (see Figure 32)
Longevity (in years)	17 (see Figure 28)	22 (see Figure 30)	12 (see Figure 32)
Response time (in years)	5 (see Figure 28)	3 (see Figure 30)	0 (see Figure 32)
Spatial extension (in km ²)	9.5 (see Figure 33a)	11.8 (see Figure 33b)	2.7 (see Figure 33c)
Estimated annual costs* (in Million €)	0.82	0.81	3.54

*Costs estimated at an inflation rate of 2.1% p.a., include seismic monitoring every 5 years for 10% of the model area, capital cost for drilling a horizontal well extension (scenario 3 only), and operational cost (including brine handling and treatment).

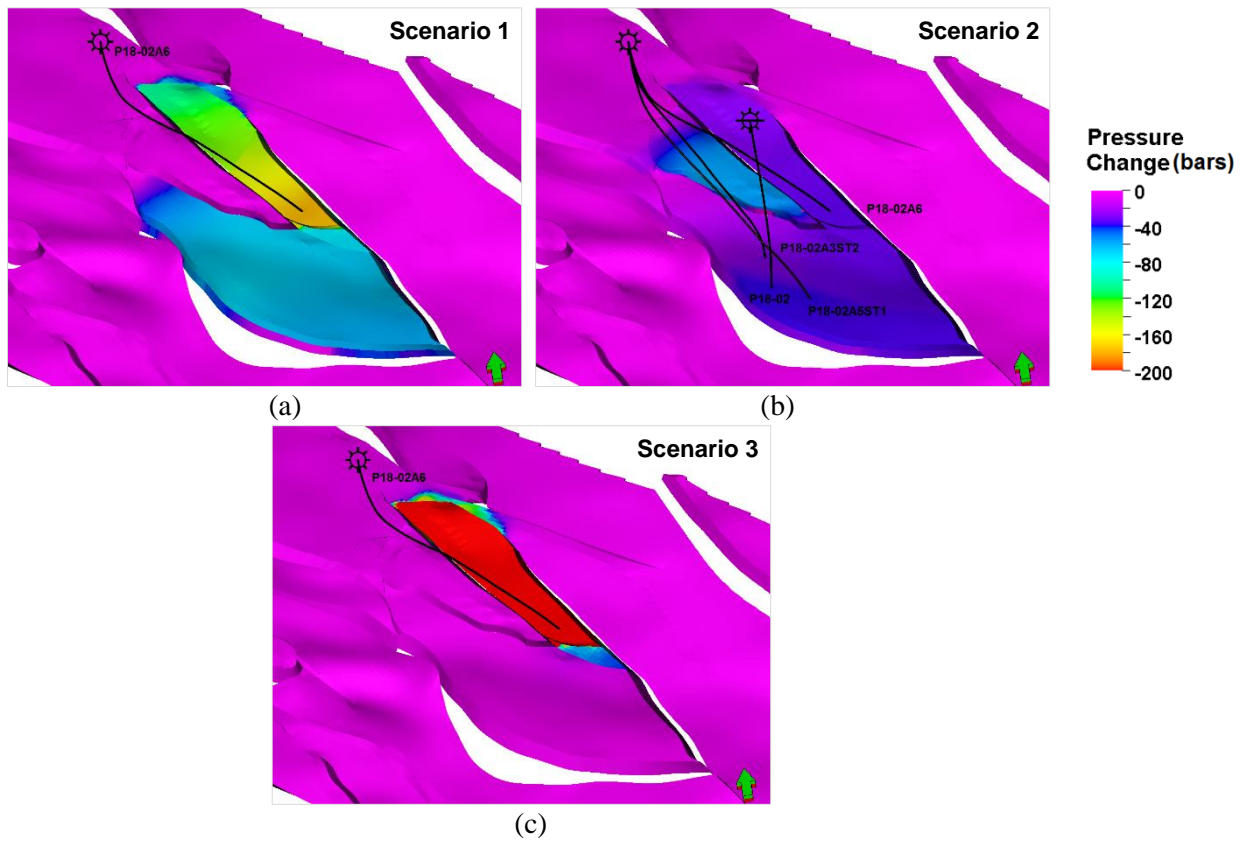


Figure 33 The footprint of pressure change indicating the area of influence of brine production: (a) CO₂ injection in compartment 18-2 (1); (b) CO₂ injection in compartment 18-2 (2); (c) CO₂ injection in compartment 18-2 (3).

4 CONCLUSIONS

In this report, the results obtained from the simulations for brine production and its assessment as a technique for CO₂ flow diversion and pressure management in a compartmentalised reservoir were presented. The factors determining the plume migration and pressure communication in the reservoir are reservoir permeability, horizontal fault transmissibility and relative pressure build-up in the compartments.

Three scenarios, namely CO₂ injection and brine production in three compartments of the P18-2 field, were considered separately. The results generally shows that the amount of flow diversion achieved is limited for the brine production layouts that were discussed. On the other hand, it is clear that there is a huge benefit of using brine production for pressure management since the associated costs could be offset by the reduction in risks induced by geomechanical failure and potentially consequent CO₂ leakage, the reduction in the area of review associated with monitoring, and the increase in storage capacity utilisation.

Further modelling work is thus required in two different aspects. One is to investigate an optimisation framework in order to maximise flow diversion of the plume considering the well layouts and CO₂ injection-brine production strategies. The other is carry out a detailed risk assessment of the strategies adopted in order to avoid early CO₂ breakthroughs at the production wells, especially in compartmentalised reservoirs.

5 REFERENCES

- Ames, R., Farfan, P. F., 1996. The environment of deposition of the Triassic Main Buntsandstein Formation in the P and Q quadrants offshore the Netherlands. In: Rondeel, H. E., Batjes, D. A. J., Nieuwenhuijs, W. H. (Eds.), *Geology of Gas and Oil under the Netherlands*. Kluwer Academic Publishers, Dordrecht, pp. 167-178.
- Apps, J. A., Zheng, L., Zhang, Y., Xu, T., Birkholzer, J. T., Evaluation of Potential Changes in Groundwater Quality in Response to CO₂ Leakage from Deep Geologic Storage. *Transport in Porous Media*, 82(1), pp. 215-246.
- Arts, R. J., Vandeweyer, V. P., Hofstee, C., Pluymaekers, M. P. D., Loeve, D., Kopp, A., Plug, W. J., 2012. The feasibility of CO₂ storage in the depleted P18-4 gas field offshore the Netherlands (the ROAD project). *International Journal of Greenhouse Gas Control*, 11, pp. S10-S20.
- Benson, S.M., 2006. Monitoring carbon dioxide sequestration in deep geological formations for inventory verification and carbon credits. *Society of Petroleum Engineers*, SPE 102833.
- Benson, S. M., Hepple, R., 2005. Prospects for early detection and options for remediation of leakage from CO₂ storage projects. *Carbon dioxide capture for storage in deep geologic formations - results from the CO₂ capture project*, 2, pp. 1189-1203.
- Bergmo, P. E. S., Grimstad, A.-A., Lindeberg, E., 2011. Simultaneous CO₂ injection and water production to optimise aquifer storage capacity. *International Journal of Greenhouse Gas Control*, 5(3), pp. 555-564.
- Birkholzer, J. T., Cihan, A., Zhou, Q., 2012. Impact-driven pressure management via targeted brine extraction - Conceptual studies of CO₂ storage in saline formations. *International Journal of Greenhouse Gas Control*, 7, pp. 168-180.
- Birkholzer, J. T., Zhou, Q., 2009. Basin-scale hydrogeologic impacts of CO₂ storage: Capacity and regulatory implications. *International Journal of Greenhouse Gas Control*, 3(6), pp. 745-756.
- Breunig, H. M., Birkholzer, J. T., Borgia, A., Oldenburg, C. M., Price, P. N., McKone, T. E., 2013. Regional evaluation of brine management for geologic carbon sequestration, *International Journal of Greenhouse Gas Control*, 14, pp. 39-48.
- Buscheck, T. A., Sun, Y., Hao, Y., Wolery, T. J., Bourcier, W., Tompson, A. F., Jones, E. D., Friedmann, S. J., Aines, R. D., 2011. Combining brine extraction, desalination, and residual-brine reinjection with CO₂ storage in saline formations: Implications for pressure management, capacity, and risk mitigation, *Energy Procedia*, 4, pp. 4283-4290.
- Buscheck, T. A., Sun, Y., Chen, M., Hao, Y., Wolery, T. J., Bourcier, B., Court, M. A., Celia, S., Friedmann, S. J., Aines, R. D., 2012. Active CO₂ reservoir management for carbon storage: Analysis of operational strategies to relieve pressure build-up and improve injectivity. *International Journal of Greenhouse Gas Control*, 6, pp. 230-245.
- Carroll, S., Hao, Y., Aines, R., 2009. Geochemical detection of carbon dioxide in dilute aquifers. *Geochemical Transactions*, 10:4.
- Court, B., Elliot, T. R., Dammel, J., Buscheck, T. A., Rohmer, J., Celia, M. A., 2011. Promising synergies to address water, sequestration, legal, and public acceptance issues associated with large-scale implementation of CO₂ sequestration. *Mitigation and Adaptation Strategies for Global Change*, 17(6), pp. 569-599.
- De Jager, J. J., 2007. Geological development. In: Wong, *et al.* (Eds.), *Geology of the Netherlands*. Royal Netherlands Academy of Arts and Sciences, Amsterdam, pp. 5-26.
- Geluk, M. C., 1999. Palaeogeographic and structural development of the Triassic in the Netherlands - new insights. In: Bachmann, G. H., Lerche, I. (Eds.), *The Epicontinental Triassic*, Zentralblatt für Geologie und Paläontologie Teil I, 1998, Heft 7-8, pp. 545-570.

- Gutierrez-Neri, M., Ganji, Z., van Breukelen, B., Kooi, H., 2012. CO₂ geological storage: injection into depleted gas fields. *The CATO-2 project*. IEAGHG Report, 2007. Remediation of leakage from CO₂ storage reservoirs. *IEA Greenhouse Gas R&D Programme*, Report No. 2007/11.
- Pagnier, H., Hofstee, C., Arts, R. J., vd Weijer, V., Loeve, D., Pluymaekers, M. P. D., Benedictus, T., 2012. The feasibility of CO₂ storage in the offshore P18 depleted gas reservoir (EEPR-ROAD). The CATO-2 project.
- Rutqvist, J., Birkholzer, J.T., Cappa, F., Tsang, C-F., 2007. Estimating maximum sustainable injection pressure during geological sequestration of CO₂ using coupled fluid flow and geomechanical fault-slip analysis. *Energy Conversion and Management*, 48(6), pp. 1798-1807.
- Rutqvist, J., Birkholzer, J.T., Tsang, C-F., 2008. Estimating maximum sustainable injection pressure during geological sequestration of CO₂ using coupled fluid flow and geomechanical fault-slip analysis. *International Journal of Rock Mechanics and Mining Sciences*, 45(2), pp. 132-143.
- Tambach, T. J., Loeve, D., Hofstee, C., Plug, W-J., Maas, J. G., 2015. Effect of CO₂ Injection on Brine Flow and Salt Precipitation after Gas Field Production. *Transport in Porous Media*, 108(1), pp. 171-183.
- Zheng, L., Apps, J.A., Zhang, Y., Xu, T., Birkholzer, J.T., 2009. On mobilization of lead and arsenic in groundwater in response to CO₂ leakage from deep geological storage. *Chemical Geology*, 268(3-4), pp. 281-297.